Optics Communications 591 (2025) 132128

Contents lists available at ScienceDirect

Optics Communications

journal homepage: www.elsevier.com/locate/optcom

All-optical generation of structured light via microwave-field-controlled spontaneous emission

M.A. Antón, E. Cabrera-Granado *

Facultad de Óptica y Optometría, Universidad Complutense de Madrid, C/ Arcos de Jalón 118, 28037 Madrid, Spain

ARTICLE INFO

Keywords:
Optical vortex
Orbital angular momentum
Coherent optical effects
Spontaneous emission

ABSTRACT

We propose a scheme for achieving spatially dependent spontaneous emission by using vortex light beams (OAM) in a five level atomic configuration. It consists of an upper excited level and four lower metastable levels. The excited level is simultaneously coupled to two ground levels by a coherent probe field and a vortex field, respectively. In addition, a microwave field couples two of the ground levels. The excited state is assumed to be coupled by the vacuum modes in the free space and eventually decays to a fifth metastable level. It is found that by manipulating key parameters such as the strength of the Laguerre–Gauss beams, the Rabi frequency and detuning of an external microwave field, and the initial state of the atoms, we can achieve highly tunable spontaneous emission spectra. A wide variety of spatiospectral behavior, including two-dimensional spectral-peak narrowing, spectral-peak enhancement and spontaneous emission quenching is obtained.

1. Introduction

In recent years there has been a growing interest in the generation, detection, propagation, and interaction of structured beams with matter due to their potential applications in particle manipulation [1,2], optical communication [3], and quantum information processing [4–6]. In most of the techniques the key feature is to use Laguerre–Gaussian (LG) modes of light which contain a helical phase term $e^{il\phi}$, where l is the topological charge (TC), and can carry orbital angular momentum (OAM) of $l\hbar$ per photon [7,8]. An important goal has been focused on obtaining structured light at a wavelength for which it is not possible to do it directly with standard optics (e.g., far-infrared or ultraviolet). In this regard the generation of coherent radiation via nonlinear optical media has been theoretically and experimentally proved using nonlinear four wave mixing process (FWM) in multi-level atomic media [9]. In such multilevel systems, laser-induced quantum coherence (QC) of atomic states can lead to quantum interference between the different excitation pathways which dramatically modifies the linear and nonlinear optical properties of the atomic medium, resulting in electromagnetically induced transparency (EIT). EIT-related processes provide a powerful and effective mechanism to control and manipulate the absorption and dispersion properties of light [10–13]. For these reasons, EIT systems have been recently proposed as good candidates to transfer and manipulate the vortex phase and intensity of the generated field of OAM via FWM processes. Different scenarios have been performed primarily in Λ three-level atoms with the control field carrying the OAM, tripod atoms [14,15] or double schemes [16–20]. For instance, the transfer of OAM between light beams based on FWM has been reported in atomic vapors and the storage of OAM has been demonstrated [21]. The helical phase twist of a generated FWM field is coherently engineered (enhanced or suppressed as desired) via the field-detuning modulation in vortex FWM processes [18,22,23]. The extension of these works to semiconductor quantum wells (SQWs) and quantum dots (QDs) is now gaining relevance due to its controllable properties such as electric dipole moments, intersubband energies and electron function symmetries, [24–26] which make these systems preferable to gaseous media for practical applications. For example, Wang et al. proposed some schemes to generate and control the spatially dependent FWM in semiconductor quantum wells [27–29], effectively modulating the helical phase of the output FWM field via multiphoton quantum interference. Besides, Hamedi et al. presented some schemes to realize the exchange and transfer of optical vortices in atomic systems [30–32]. Chao et al. [33] proposed a theoretical scheme to manipulate the helical phase via ultraslow FWM in a six-level atomic system driven by a field with OAM and making use of two EIT control fields. Zhang et al. [20] proposed an efficient scheme to manipulate the perfect optical vortex (POV) beam in a cold atomic ensemble with a five-level configuration where the OAM can be completely transferred from a POV control beam to the generated mixing field via inelastic FWM process. Optical vortex of a control field can also be

* Corresponding author.
E-mail addresses: antonm@ucm.es (M.A. Antón), ecabrera@ucm.es (E. Cabrera-Granado).

https://doi.org/10.1016/j.optcom.2025.132128
Received 11 March 2025; Received in revised form 2 June 2025; Accepted 15 June 2025
Available online 7 July 2025

transferred to a generated probe beam via Raman processes [34] and in other more sophisticated systems such as molecular magnets [35] and graphene [36].

In addition to the coherent generation of structured light, the incoherent properties of atoms can be correspondingly modulated via the light fields as well. For example, the spontaneous emission, due to the atomic interaction with environmental modes, can be controlled or even canceled due to laser field induced quantum interferences [37,38]. The physical essentials of atomic coherence effects can be attributed to laser induced dressed states as well as quantum interference resulting from different transitions pathways. Several theoretical proposals of atomic systems have appeared where coupling to one or more coherent fields allow the management of the features of the fluorescence spectrum [39], spontaneously generated coherence [40], cancellation of spontaneous emission by quantum interference [40–44] and by placing atoms into different reservoirs, such as in optical cavities [45], photonic crystals [46] and in proximity to plasmonic nanostructures [47], which have different densities of modes interacting with the atoms. Therefore the possibility of shaping the spontaneous emission spectrum via control fields opens a new avenue for achieving spatio-spectral control over spontaneous emission and the generation of structured light via spontaneous emission in sharp contrast to the FWM techniques described above.

It should be noted that the generation of structured light via spontaneous emission have been analyzed very recently using M-type [48] and V-type atoms [49]. In both atomic systems two nearly degenerate upper states decay to a common metastable state given place to vacuum induced coherence (VIC) which appears as a crucial ingredient to obtain spatially structured light. However, it is well known that the existence of this quantum interference requires that two close-lying levels be nearly degenerate and that the atomic dipole moments be nonorthogonal when the atom is placed in free space. Unfortunately, finding an experimentally feasible atomic system with VIC is challenging, therefore limiting their applications for common quantum systems such as atoms and molecules [38].

In order to circumvent this problem, here we present an alternative for the generation of spatially dependent spontaneously emission by using vortex light beams (OAM) interacting with a five-level atomic configuration where a control microwave field modulates the spontaneous emission from an excited state to a metastable state. The presence of the control and microwave fields dressed the atom, leading to three close-lying dressed states. Thus, before atoms spontaneously decay to the metastable level, they can go through three different pathways and the observed singular spontaneous emission spectra can be viewed as results of multiple VIC in the dressed-state picture [50]. The main advantage is that VIC is produced between dressed states not real states. Related work to the present study has been performed by Abbas et al. [51] who quite recently studied the generated spatially structured spontaneously emission in an atomic four-level configuration comprising two lower states, as well as two upper states interacting with three fields and creating a closed-loop atomic configuration. The generated spatially structured spontaneously emission does not rely on the quantum interference of spontaneous emission. In this context our scheme represents a similar approach to obtain structured spontaneous emission without the presence of vacuum induced coherence. It is worth noting that our system shows some advantages, as it does not impose any conditions on the detunings of the different fields. On the contrary, Abbas's system has the interesting property of being able to control the spontaneous emission via the relative phase of the fields. In any case, both systems could be more suitable from an experimental point of view than previously proposed schemes.

The paper is organized as follows: Section 2 establishes a model to describe the five-level atom interacting with probe, and coupling fields. From that we derive an effective Hamiltonian which allows us to obtain the dynamical equations of the matrix density elements of the atomic system. In Section 3, we explore the generation of structured light via spontaneous emission process and discuss the effects of the intensity and detuning of the control fields on the spatial modulation of spontaneous emission. Finally, Section 4 summarizes our main conclusions.

2. Theoretical model and equations

We consider a medium of five-level atoms consisting of three lower levels $|0\rangle$, $|1\rangle$, and $|2\rangle$, an excited state $|3\rangle$, and a metastable level $|e\rangle$ as shown in Fig. 1(a). An equivalent dressed system is displayed in Fig. 1(b).

This atomic system can be obtained by using the hyperfine states of ^{87}Rb [52]. The atom is interacting with a probe field with carrier frequency ω_p and Rabi frequency Ω_p which couples the transition $|0\rangle \rightarrow |3\rangle$. The transition $|2\rangle \rightarrow |3\rangle$, is driven by a cw control field with carrier frequency ω_c and Rabi frequency Ω_c. In addition the transition $|1\rangle \rightarrow |2\rangle$ is driven by a microwave field with frequency ω_m and Rabi frequency Ω_m. The upper level $|e\rangle$ decays to the metastable state $|e\rangle$ via interactions with the vacuum field modes in the free space. The OAM field Ω_c is assumed to be in the form of a vortex Laguerre–Gaussian (LG) field

$$\Omega_c(r,\varphi) = \Omega_{c0}\sqrt{\frac{2p!}{\pi(p+l)!}}\frac{1}{w_0}\left(\frac{\sqrt{2}r}{w_0}\right)^{|l|} L_p^{|l|}\left(\frac{2r^2}{w_0^2}\right) e^{\frac{-2r^2}{w_0^2}} e^{-il\phi}. \tag{1}$$

Here Ω_{c0} is the initial Rabi frequency of the LG field, r is the radial coordinate, w_0 is the beam waist, and $L_p^{|l|}$ is the Laguerre polynomial.

The resonant frequencies between the different levels are $\omega_{ij} = \omega_i - \omega_j$, $|j\rangle$ $(j = 0-3)$. Therefore, under the electric-dipole and rotating-wave approximations, the interaction Hamiltonian for the five-level system can be described by

$$\begin{aligned} H &= \hbar\left[\Delta_p\sigma_{33} + (\Delta_p - \Delta_c)\sigma_{22} + (\Delta_p - \Delta_c - \Delta_m)\sigma_{11} + (\Delta_p - \delta_k)\sigma_{ee}\right] \\ &\quad + \hbar\left(\Omega_p\sigma_{30} + \Omega_c\sigma_{32} + \Omega_m\sigma_{21} + H.c.\right) \\ &\quad + \hbar\sum_{k\lambda} g_{k\lambda}b_{k\lambda}e^{i(\Delta_p-\delta_k)t}\sigma_{3e} + \hbar\sum_{k\lambda} g_{k\lambda}^* b_{k\lambda}^+ e^{-i(\Delta_p-\delta_k)t}\sigma_{e3}, \end{aligned} \tag{2}$$

where H.c. is the abbreviation for the Hermitian conjugate. Here, $\sigma_{mn} = |m\rangle\langle n|$ are the usual Pauli matrices, $b_{k\lambda}$ and $b_{k\lambda}^+$ correspond to the creation and annihilation operators of reservoir modes with angular frequency $\omega_{k\lambda}$ with polarization $\vec{e}_{k\lambda}$ $(\lambda = 1,2)$. The parameter $g_{k\lambda}$ is the coupling constant of the atomic transition $|3\rangle \rightarrow |e\rangle$ with the electromagnetic vacuum mode and is given by

$$g_k = \sqrt{\frac{\omega_{k\lambda}}{2\hbar\epsilon_0 V}}(\vec{\mu}_{3e}\cdot\vec{e}_{k\lambda}), \tag{3}$$

In this context, $\vec{e}_{k\lambda}$ denotes the electrically polarized vector corresponding to the released photon with frequency $\omega_{k\lambda}$, $\vec{\mu}_{3e}$ is the transition dipole moment associated with the transition $|3\rangle \rightarrow |e\rangle$, and V accounts for the quantified volume. The Rabi frequencies of corresponding fields are defined in terms of the dipole moment μ_{ij} between the atomic levels $|i\rangle$ and $|j\rangle$ and the amplitude of the electric field applied to this transition E_j $(j = p,c,m)$ as $\Omega_p = \vec{\mu}_{03}\cdot\vec{E}_p/(2\hbar)$, $\Omega_c = \vec{\mu}_{23}\cdot\vec{E}_c/(2\hbar)$, and $\Omega_m = \vec{\mu}_{12}\cdot\vec{E}_m/(2\hbar)$. The detunings appearing in Eq. (2) are defined as $\Delta_p = \omega_{30} - \omega_p$, $\Delta_m = \omega_{21} - \omega_m$, $\Delta_c = \omega_{32} - \omega_c$, and $\delta_k = \omega_{3e} - \omega_k$.

Since we assume that state $|e\rangle$ is a metastable state, the system can remain in this state for a relatively long time before decaying to a lower energy state. Thus the dynamics of this system can be described by the probability amplitude equations through deploying the state vector as

$$|\Psi(r)\rangle = a_0(t)|0\rangle|0_k\rangle + a_1(t)|1\rangle|0_k\rangle + a_2(t)|2\rangle|0_k\rangle + a_3(t)|3\rangle|0_k\rangle + \sum_k a_k(t)|e\rangle|1_k\rangle, \tag{4}$$

where the probability amplitude $a_j(t)$ $(j = 0_3)$ represents the temporary weight of each case without the photon emitted into the kth vacuum mode, i.e., labeled by $|0_k\rangle$, while $a_k(t)$ represents the probability of

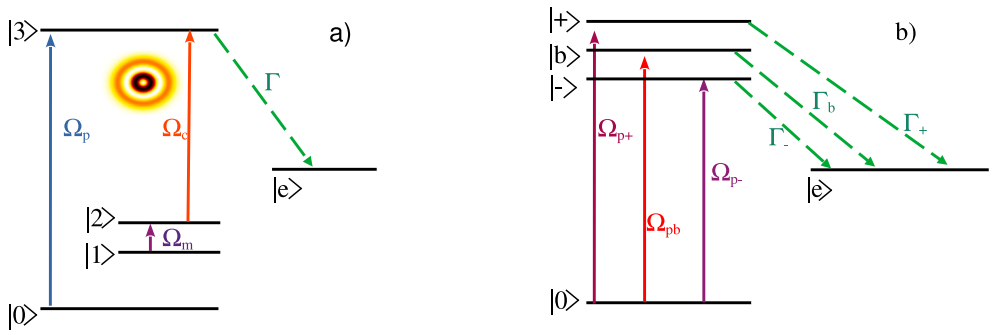

Fig. 1. Schematic diagram (a) of the five-level atomic system. Transitions $|0\rangle \to |3\rangle$ and $|2\rangle \to |3\rangle$ are coupled by a probe field Ω_p and a control field Ω_c, respectively. This control field is a vortex Laguerre–Gaussian (LG) field. In addition, a rf-driving field Ω_m couples the magnetically dipole allowed transition $|1\rangle \to |2\rangle$. Atom-field picture (b) of the same system in the dressed basis of the control and microwave fields Ω_c and Ω_m, showing the interfering three decay channels to $|e\rangle$ state. A derivation of the equations of motion in the dressed-states basis is explained in the Appendix.

the atom on the metastable state $|e\rangle$ with one photon emitted in the kth vacuum mode. Here, we would like to point out that we have not considered relaxation from excited states $|3\rangle$ to the ground states $|0\rangle$ and $|2\rangle$. The incorporation of decay channels from the excited states to the ground state introduces decoherence, diminishing coherence among $|0\rangle$, $|2\rangle$ and $|3\rangle$, which may diminish interference effects in the emission spectrum. However, the results are expected to be physically the same.

Making use of Schrödinger equation in the interaction picture, the coupled equations of motion for the probability amplitudes $a_j(t)$ can be readily obtained as:

$$\begin{aligned}
\frac{\partial a_0(t)}{\partial t} &= -i\Omega_p^* a_3(t),\\
\frac{\partial a_1(t)}{\partial t} &= -i\left(\Delta_p - \Delta_c - \Delta_m\right) a_1(t) - i\Omega_m^* a_2(t),\\
\frac{\partial a_2(t)}{\partial t} &= -i\left(\Delta_p - \Delta_c\right) a_2(t) - i\Omega_c^* a_3(t) - i\Omega_m a_1(t)\,,\\
\frac{\partial a_3(t)}{\partial t} &= -\left[\Gamma/2 + i\Delta_p\right] a_3(t) - i\Omega_p a_0(t) - i\Omega_c a_2(t)\,,\\
\frac{\partial a_k(t)}{\partial t} &= -i\left(\Delta_p - \delta_k\right) a_k(t) - ig_k^* a_3(t)\,,
\end{aligned} \tag{5}$$

where Γ is the spontaneous decay rate from level $|3\rangle$ to the metastable state $|e\rangle$.

By applying Laplace transformations $\hat{a}_j(s) = \int a_j(t)e^{-st}dt, (j = 0-3)$, to Eq. (5), we obtain

$$\begin{aligned}
s\hat{a}_0(s) - a_0(0) &= -i\Omega_p^* \hat{a}_3(s),\\
s\hat{a}_1(s) - a_1(0) &= -i\left(\Delta_p - \Delta_c - \Delta_m\right)\hat{a}_1(s) - i\Omega_m^* \hat{a}_2(t),\\
s\hat{a}_2(s) - a_2(0) &= -i\left(\Delta_p - \Delta_c\right)\hat{a}_2(s) - i\Omega_c^* \hat{a}_3(t) - i\Omega_m \hat{a}_1(s)\,,\\
s\hat{a}_3(s) - a_3(0) &= -\left[\Gamma/2 + i\Delta_p\right]\hat{a}_3(s) - i\Omega_p a_0(s) - is\Omega_c \hat{a}_2(s)\,,\\
s\hat{a}_k(s) - a_k(0) &= -i\left(\Delta_p - \delta_k\right)\hat{a}_k(s) - ig_k^* \hat{a}_3(s)\,.
\end{aligned} \tag{6}$$

Eqs. (6) can be solved in terms of initial conditions $a_j(0), (j = 0-3)$. The solution of amplitude $\hat{a}_3(s)$ can be found as

$$\hat{a}_3(s) = \frac{f_0(s)a_0(0) + f_1(s)a_1(0) + f_2(s)a_2(0) + f_3(s)a_3(0)}{f(s)}. \tag{7}$$

Here,

$$\begin{aligned}
f_0(s) &= -i\Omega_p\left[(s+iw_1)(s+iw_2) + |\Omega_m|^2\right],\\
f_1(s) &= -s\Omega_c\Omega_m,\\
f_2(s) &= -is(s+iw_1)\Omega_c,\\
f_3(s) &= s\left[(s+iw_1)(s+iw_2) + |\Omega_m|^2\right],\\
f(s) &= s(s+iw_3)\left[(s+iw_1)(s+iw_2) + |\Omega_m|^2\right]\\
&\quad + \left[(s+iw_1)(s+iw_2) + |\Omega_m|^2\right]|\Omega_p|^2 + s(s+iw_1)|\Omega_c|^2\,,
\end{aligned} \tag{8}$$

where we have introduced the definitions $w_1 = \Delta_p - \Delta_c - \Delta_m$, $w_2 = \Delta_p - \Delta_c$, $w_3 = \Delta_p - i\frac{\Gamma}{2}$, and $w_4 = \Delta_p - \delta_k$.

As a result, the atom can oscillate between its ground state $|0\rangle$ and the excited state $|3\rangle$ in short-time evolution; however, it would eventually decay to the metastable state $|e\rangle$ due to the spontaneous emission in the long-time limit, i.e., $a_0(t \to \infty) = a_1(t \to \infty) = a_3(t \to \infty) = a_3(t \to \infty) = 0$. Hence, the spontaneous emission spectrum in the long-time limit [53] is

$$S(\delta_k) = \frac{\Gamma}{2\pi}|a_k(t \to \infty)|^2\,. \tag{9}$$

According to Eq. (6), we have $\hat{a}_k(s) = \frac{-ig_k^*\hat{a}_3(s)}{s+iw4}$. Then, by using the inverse Laplace transformation and the final-value theorem [53] we finally obtain the spontaneous emission spectrum as

$$\begin{aligned}
S(\delta_k) &= \frac{\Gamma}{2\pi}|a_k(t \to \infty)|^2 = \frac{\Gamma}{2\pi}|\hat{a}_3(s = -iw_4)|^2\\
&= \left|\frac{f_0(\delta_k)a_0(0) + f_1(\delta_k)a_1(0) + f_2(\delta_k)a_2(0) + f_3(\delta_k)a_3(0)}{f(\delta_k)}\right|^2,
\end{aligned} \tag{10}$$

where

$$\begin{aligned}
f_0(\delta_k) &= i\Omega_p\left[(w_4 - w_1)(w_4 - w_2) - |\Omega_m|^2\right],\\
f_1(\delta_k) &= iw_4\Omega_c\Omega_m,\\
f_2(\delta_k) &= iw_4(w_4 - w_1)\Omega_c,\\
f_3(\delta_k) &= iw_4\left[(w_4 - w_1)(w_4 - w_2) - |\Omega_m|^2\right],\\
f(\delta_k) &= w_4(w_4 - w_3)\left[(w_4 - w_1)(w_4 - w_2) - |\Omega_m|^2\right]\\
&\quad - \left[(w_4 - w_1)(w_4 - w_2) - |\Omega_m|^2\right]|\Omega_p|^2 - w_4(w_4 - w_1)|\Omega_c|^2
\end{aligned} \tag{11}$$

Eq. (10) gives the spontaneously emitted field at an arbitrary frequency. It can be seen that the spontaneous output field can inherit the characteristics of the control fields, i.e. it can be modulated via the Rabi frequency, detunings and the charge number of the OAM vortex beams. In the following we will analyze the influence of these parameters on the generation of structured light by the control of spontaneous emission.

3. Numerical results and discussion

For illustration of the numerical results, we choose a realistic system consisting in ^{87}Rb [52,54]. The simplified level configuration is shown in Fig. 1. The different atomic levels considered are the following: $|0\rangle = |5S_{1/2}, F = 1, m_F = 1\rangle$, $|1\rangle = |5S_{1/2}, F = 1, m_F = 0\rangle$, $|2\rangle = |5S_{1/2}, F = 2, m_F = 0\rangle$, $|3\rangle = |5P_{3/2}, F = 2, m_F = 1\rangle$, and $|e\rangle = |5S_{1/2}, F = 2, m_F = 2\rangle$. The microwave field couples the dipole transition between $|1\rangle$ and $|2\rangle$ with a splitting frequency $\omega_{21} = 6.84$ GHz. The transition from the excited state $|3\rangle$ to the metastable level $|e\rangle$ can be coupled by the vacuum modes in free space.

Before proceeding with the generation of structured light, we briefly focus on the influence of the different external parameters on the emission spectrum. In order to better discriminate the effect of each of these

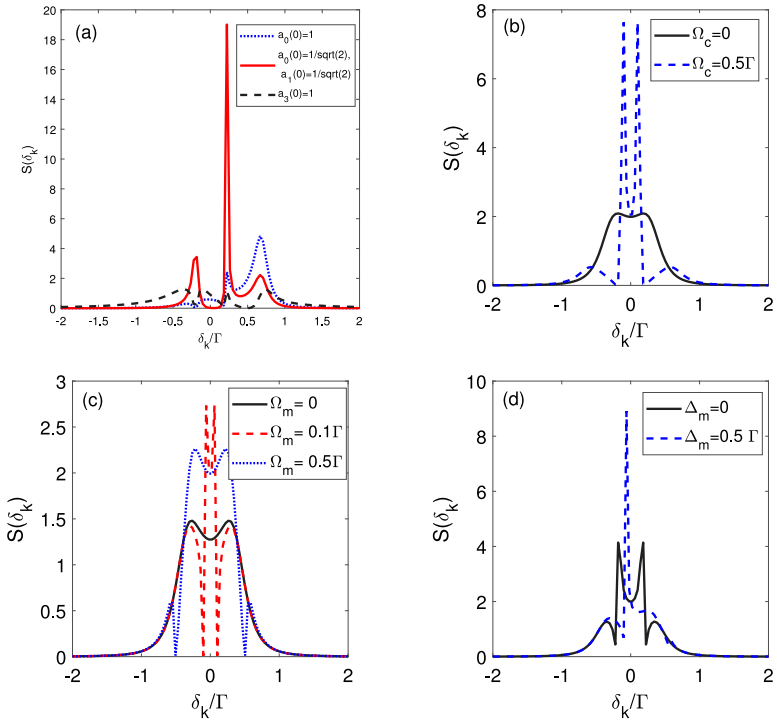

Fig. 2. Spontaneous emission spectrum versus the detuning δ_k of radiated light for (a) different initial superposition states; (b) different constant values of Ω_c; (c) effect of microwave Rabi frequency Ω_m, and (d) effect of microwave detuning Δ_m. The remaining parameters are as follows $\Omega_p = 0.4\Gamma$, $\Omega_c = 2\Gamma$, $\Delta_p = \Delta_c = 0$.

parameters, here we will restrict to a fixed, i.e. spatially homogeneous, field Ω_c. Therefore, no spatial dependence of the spontaneous emission spectrum is considered so far. First we analyze in Fig. 2 the role of the initial probability amplitudes on the spontaneous spectra $S(\delta_k)$. Fig. 2(a) displays the spontaneous emission spectrum versus detuning by initially preparing the atom on its ground state, i.e., $a_0(0) = 1$, $a_1(0) = a_2(0) = a_3(0) = 0$ and while $\Delta_p = 0.2\Gamma$, $\Delta_c = \Delta_m = 0$. From Fig. 2(a), one can clearly note that the spontaneous emission mainly occurs at one side band (dotted line).

For the case that the atom is in a superposition state, namely, $a_0(0) = a_1(0) = 1/\sqrt{2}$ and $a_2(0) = a_3(0) = 0$ (dashed line) the spectrum shows a well developed Mollow triplet with a very high and ultranarrow central peak at $\delta_k = \Delta_p$ (solid line). Finally, if the atom is initially prepared in the excited state, i.e., $a_3(0) = 1$ and $a_0(0) = a_1(0) = a_2(0) = 0$ (dotted line), quenching of the spontaneous emission is observed.

Now we analyze the effects of external parameters such as the Rabi frequency of the control field, Ω_c, and the Rabi frequency and detuning of the microwave field. For simplicity we assume that the atom is initially in the ground state ($a_0 = 1$) and the probe, coupling and microwave fields are respectively tuned to the corresponding transitions, i.e. $\Delta_p = \Delta_c = \Delta_m = 0$. The solid line of Fig. 2(b) shows that in absence of control field ($\Omega_c = 0$), the spectrum develops a peak structure. However when $\Omega_c = 0.5\Gamma$ two ultranarrow lines appears on both sides of zero detuning of δ_k. In addition, there are two points where spontaneous emission is quenched. The position of these points can be controlled with the Rabi frequency of the control field.

Next, we focus on the variation of emission spectrum when the microwave field, Ω_m is changed. Fig. 2(c) shows that a similar behavior as in the previous case appears. For $\Omega_m = 0$, the emission spectrum exhibits a symmetrical double-peak structure (solid line), while a splitting occurs when $\Omega_m = 0.1\Gamma$, given place to a four-peak structure. A further increase of the Rabi frequency to $\Omega_m = 0.5\Gamma$ simply broadens the spectrum. As can be seen, the change of the microwave field intensity affects appreciably both the width and the height of the spectral lines. Finally in Fig. 2(d) we plot the spontaneous emission spectrum $S(\delta_k)$ versus the detuning δ_k by modulating the detuning Δ_m of the external microwave field under the same initial conditions as above. It is clearly shown that, when the external coherent microwave field is tuned to level $|2\rangle (i.e., \Delta_m = 0)$ (solid line), a symmetric spectrum appears. Interestingly, for a small frequency detuning of the external coherent microwave field, i.e., $\Delta_m = 0.5\Gamma$ (dashed line), one side ultranarrow peak is quenched while an ultranarrow side line is enhanced.

The physical reason for the variation of the spectral-lines number shown in Fig. 2 can be qualitatively understood by invoking the dressed-state basis generated by the control and microwave field. In our numerical calculation (see Appendix), we find the three eigenvalues as λ_b, λ_+, and λ_- which depend on Rabi frequencies and detuning of the driven fields. As shown in Fig. 1 the bare state $|3\rangle$ is split in three dressed-state sublevels $|\pm\rangle$ and $|b\rangle$. The spontaneous emission occurs from these sublevels to the metastable level $|e\rangle$. From the dynamical equations of these sublevels (see Appendix) it can be seen that there exists quantum interference between three different spontaneous emission pathways $|+\rangle \rightarrow |e\rangle$, $|b\rangle \rightarrow |e\rangle$, and $|-\rangle \rightarrow |e\rangle$, so we can conclude that the spontaneous emission spectrum should be generally composed of three peaks. These multiple competitive transition pathways result in spectral-line narrowing, spectra-line enhancement, spectral-line suppression, and quenching in the spontaneous emission spectra.

In conclusion, these results clearly show that, by properly adjusting the initial probability amplitudes, the detuning, and the Rabi frequency of the control and/or the microwave field, we can modulate the spontaneous emission spectrum, allowing spectral-line narrowing, spectral-line enhancement, and spectral-line suppression. These facts can allow spatiospectral control of spontaneous emission when OAM fields Ω_c drive the atom. In the following section we will analyze this question.

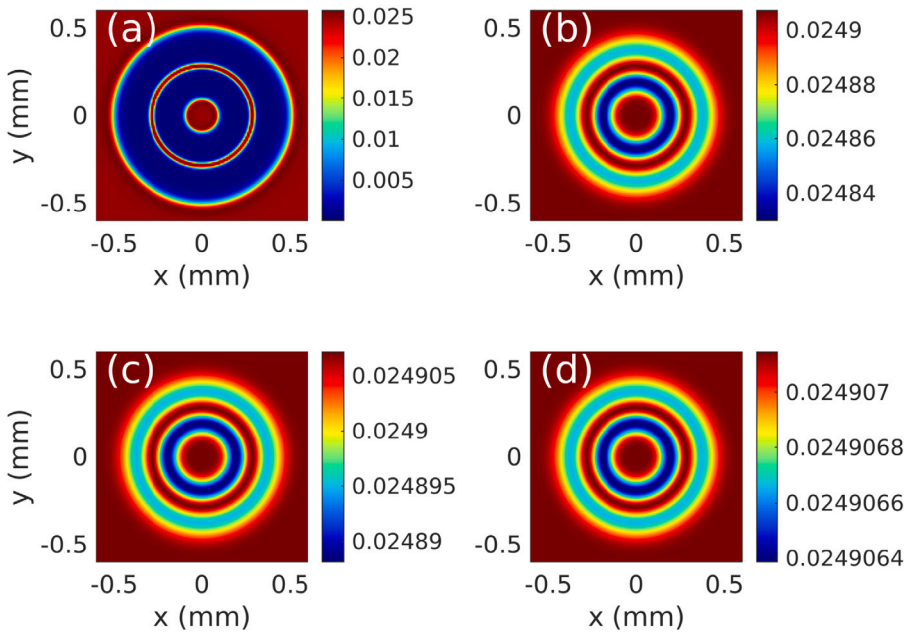

Fig. 3. Spatial modulation of the spontaneous emission $S(\delta_k)$ for initial condition $a_0(0) = 1$, $a_1(0) = 0$, $a_2(0) = 0$, $a_3(0) = 0$, and different Rabi frequencies of the microwave field Ω_m:(a) $\Omega_m = 0$, (b) $\Omega_m = 0.5\Gamma$, (c) $\Omega_m = \Gamma$, and (d) $\Omega_m = 5\Gamma$. Other parameters are $\delta_k = 0.04\Gamma$, $\Omega_p = 0.4\Gamma$, $\Omega_c = \Gamma$, $\Omega_m = 0.2\Gamma$; $\Delta_p = 2\Gamma$, $\Delta_c = 0$, and $\Delta_m = 0$ and topological charge $l = 4$.

3.1. One LG-mode control beam

Let us now examine the spatially dependence of the spontaneous emission spectrum when a spatially structured control field Ω_c given in Eq. (1) is injected. Eq. (10) and Fig. 2(a) show that the spontaneous emission spectrum is very sensitive to the initial conditions of the atomic state. In the following we will analyze the key role of the microwave field to spatially modulate the spontaneous emission in two scenarios: In the first, the atom is initially prepared in the ground state $|0\rangle$. Then we will consider the case of an initial superposition between $|0\rangle$ and $|1\rangle$ states.

Fig. 3 displays several examples of the spatial dependence of the emitted light for different values of the microwave control field Ω_m and for a LG-mode beam with $p = 1$ and $l = 4$ as the control field. We can see that the intensity profiles develop a regular doughnut shape which is consistent with the typical feature of a standard LG beam, and most importantly, the influence of Ω_m is negligible, only causing slight changes in emission intensity. No effects of the OAM phase are observed. Thus the spontaneous spectrum depends only the intensity distribution of the applied fields.

Now we consider the second scenario in which the atoms are initially on a superposition state, i.e., $a_0(0) = 1/\sqrt{2}$, $a_1(0) = 1/\sqrt{2}$, $a_2(0) = a_3(0) = 0$. Besides, we consider a LG beam with $p = 1$ and $l = 4$, while we set $\delta_k = 0.3\Gamma$. We can see that the change on the initial probability amplitudes dramatically modifies the spatial distribution on the spontaneous spectrum and more remarkably, the spatial pattern of emission can be modulated by the Rabi frequency of the microwave field, as evidenced in Fig. 4(a)–(d). Fig. 4(a) shows a doughnut-shape of the spontaneous emission profile for $\Omega_m = 0$, with near-zero intensity at the center. However, with the presence of the microwave field some features of the OAM control field emerges. Thus, for $\Omega_m = 0.001\gamma$, we can see in Fig. 4(b), the appearance of four enhanced regions within the rings. When $\Omega_m = 0.01\Gamma$ (see Fig. 4(c)) the 4-fold symmetry in the spatial spectrum is evident, where four dark-red structures denote positions of spontaneous emission enhancement or 2D spectral peaks, while the blue areas correspond to regions causing quenching or reduction in spontaneous emission in the 2D azimuthal plane. If the intensity of the microwave field is further increased to $\Omega_m = 5\Gamma$, a petal-like structure arises with well defined spatial regions of enhanced or quenched spontaneous emission.

The behavior displayed in Figs. 3 and 4 can be better understood by a closer inspection of Eqs. (10) and (11). In effect, by incorporating in those equations the initial conditions $a_2(0) = a_3(0) = 0$, i.e., no initial populations in levels $|2\rangle$ and $|3\rangle$, the spontaneous emission spectrum can be expressed as

$$S(\delta_k) = \frac{1}{2}\left|\frac{f_0(s)a_0(0) + f_1(s)a_1(0)}{f(s)}\right|^2. \tag{12}$$

For the case of initial condition $a_0(0) = 1$ (atom initially in the ground state) considered in Fig. 3, and taking into account the particular values $\Delta_c = \Delta_m = 0$, Eq. (12) can be approximated by

$$S(\delta_k) \simeq \frac{1}{2}|\Omega_p|^2\left|\frac{(\delta_k^2 - |\Omega_m|^2)}{(\delta_k^2 - |\Omega_m|^2)(\delta_k^2 - |\Omega_p|^2 - \delta_k^2|\Omega_c|^2)}\right|^2. \tag{13}$$

We can find from Eq. (13) that the spontaneous emission spectrum only depends significantly on the intensity distribution of the applied driving fields. In this case, we have only a spatial distribution of the spontaneous emission spectrum without any dependence on Ω_c phase. In addition, the role of Ω_m is restricted to a smooth change on the intensity spatial profile of $S(\delta_k)$.

However, in the case in which the system is initially in the superposition state $a_0(0) = 1/\sqrt{2}$, $a_1(0) = 1/\sqrt{2}$, $a_2(0) = a_3(0) = 0$, as in Fig. 4, the term $f_1(\delta_k)a_1(0) = i\omega_4\Omega_c\Omega_m a_1(0)$ with $\omega_4 = \Delta_p - i\Gamma/2$ carries information of the control field-phase on the spatial structure of the spontaneous emission spectrum . In this case, Eq. (12) can be roughly approximated as

$$S(\delta_k) = \frac{1}{4}\left|\frac{\Omega_p(\delta_k^2 - |\Omega_m|^2) + (\Delta_p - \delta_k)\Omega_c\Omega_m}{(\delta_k^2 - |\Omega_m|^2)(\delta_k^2 - |\Omega_p|^2 - \delta_k^2|\Omega_c|^2)}\right|^2, \tag{14}$$

It must be noted that $f(\delta_k)$ also contains a contribution of the control field, but through its intensity $|\Omega_c|^2$. By developing the numerator of the Eq. (14) it can be seen that an interference term emerges that is proportional to the product $\Omega_p(\Omega_c + \Omega_c^*)\Omega_m \sim \Omega_p\Omega_m\Omega_{c0}\cos(l\phi)$. This term is crucial for the generation of structured light and clearly shows the coupling between the microwave field and the OAM field. In fact

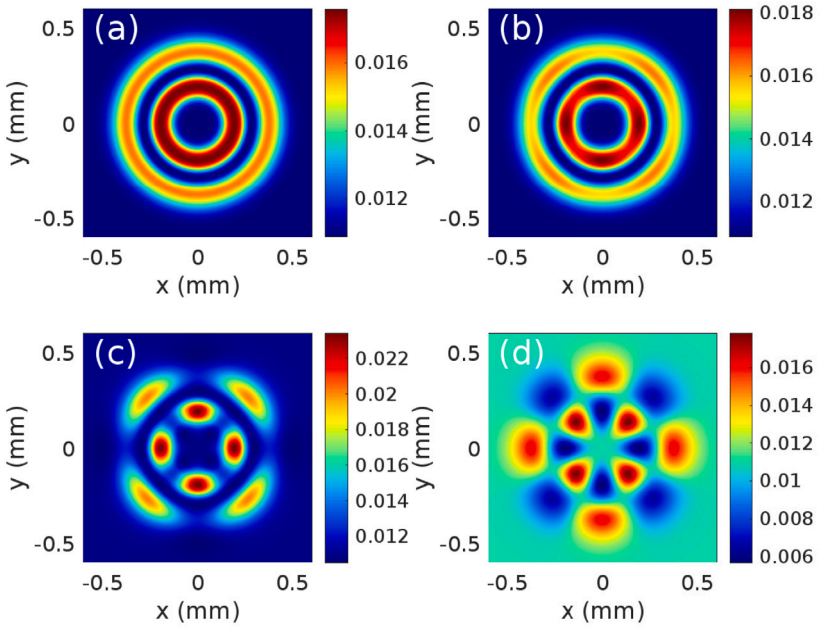

Fig. 4. Spatial modulation of the spontaneous emission $S(\delta_k)$ for initial condition $a_0(0) = 1/\sqrt{(2)}$, $a_1(0) = 1/\sqrt{(2)}$, $a_2(0) = 0$, $a_3(0) = 0$, and different values of the Rabi frequency of the microwave field: (a) $\Omega_m = 0$, (b) $\Omega_m = 0.001\Gamma$, (c) $\Omega_m = 0.01\Gamma$, and (d) $\Omega_m = 5\Gamma$. Other parameters $\delta_k = 0.3\Gamma$, $\Omega_p = 0.4\Gamma$, $\Omega_c = \Gamma$, $\Delta_p = 2\Gamma$ and $\Delta_c = \Delta_m = 0$.

if the microwave field Ω_m is canceled, the phase dependence of the emission spectrum disappears.

Therefore, the topological charge of the OAM can be used to spatially modulate the spontaneous emission spectrum. Fig. 5 displays the spatial patterns of the spontaneous emission keeping the same configuration as in Fig. 4, but changing the topological charge of the OAM, with specific cases illustrated as (a) $l = 1$, (b) $l = 2$, (c) $l = 3$, and (d) $l = 4$, and $p = 1$ for all cases. We can see that the change on the initial probability amplitudes dramatically modifies the spatial distribution on the spontaneous spectrum. As evidenced in Fig. 5(a)–(d), different OAM values lead to distinct patterns in the position-dependent spontaneous emission profiles. The red bright area within each petal represents maximum values of spontaneous emission, i.e., the atom is emitting light with high probability in those regions. On the other hand, blue regions in the depicted patterns correspond to quenching of spontaneous emission, indicating that little light is being emitted in those areas. Moreover, from Fig. 5, one can also observe that the high-probability emission ring presents an l-fold symmetry. This symmetry arises due to the spatial distribution of spatially engineered quenched and enhanced spontaneous emission regions in the medium as a result of quantum interference in spontaneous emission.

Clearly, we can conclude that some characteristics of the incident vortex beam can be transferred to the generated spontaneous emission.

Although some related schemes were recently proposed to investigate the generation of optical vortices through spontaneous emission spectra using M-type atom [48] or V-type atom [49], the current system offers some more control possibilities. Comparing with those schemes, the major feature of our proposal is that not vacuum induced coherence is necessary to obtain interferences in spontaneous emission spectra.

A variety of spontaneous emission patterns can also be obtained by changing the detuning of the microwave field, some of them can be seen in Fig. 6 where we have depicted spatial profile of the spontaneous emission spectrum $S(\delta_k)$ by modulating the detuning Δ_m of the external microwave field, in this case, for $\delta_k = 0$. It is clearly shown that again the spatial features of the OAM field are transferred to the emission spectrum.

Here, it should be emphasized that the obtained results provide a clue for engineering the spatial emission profile via changing the Rabi frequency and detuning of the microwave field and the topological charge of the vortex beam. Thus, in our scheme we take advantage of the additional degrees of freedom provided by the Rabi frequency and detuning of the microwave field.

3.2. Two LG-mode control beams

In this section, we turn to the scenario in which both of the probe and control fields are LG-mode beams. We will show that emergent patterns of the spontaneous emission spectrum can be observed through tuning the value of topological charges l_1 and l_2 of Ω_p and Ω_c, respectively.

Let us first consider the case of symmetric helicity drivings (i.e., $l_1 = l_2$) and we assume that $\Delta_c = \Delta_m = 0$. As previously stated, the atom is initially at the superposition state $a_1(0) = 1/\sqrt{2}$, $a_2(0) = 1/\sqrt{2}$, $a_3(0) = 0$. Fig. 7 shows the spatially distributed portions of the spontaneous emission spectrum $S(\delta_k)$ at various OAM values.

The profile of spontaneous emission reveals a regular doughnut-shape emission ring as in the case of one-OAM field, with an increasing radius with the OAM number.

This behavior can be analyzed again from Eq. (10). For the considered case in Fig. 7, $\Delta_c = \Delta_m = 0$, so we have $w_1 = w_2 = \Delta_p$, $w_3 = \Delta_p - i\Gamma/2$ and $w_4 = \Delta_p - \delta_k$. With these parameters, Eq. (10) becomes

$$S(\delta_k) = \frac{1}{2}\left|\frac{A\Omega_p + B\Omega_c}{f(\delta_k)}\right|^2$$
$$= \frac{1}{2}\left|\frac{A^2|\Omega_p(l_1)|^2 + B^2|\Omega_c(l_2)|^2 + 2AB|\Omega_p(l_1)||\Omega_c(l_2)|\cos\left[(l_1 - l_2)\Phi\right]}{f(\delta_k)}\right|^2, \quad (15)$$

where $A = \delta_k^2 - |\Omega_m|^2$, and $B = (\Delta_p - \delta_k)|\Omega_m|$. We can see that in the case of equal topological charges $l_1 = l_2$, the interference term $\cos\left[(l_1 - l_2)\Phi\right]$ is not modulated, which leads to a non-modulated spontaneous emission profile.

Next, we will explore cases beyond symmetric helicity (i.e., $l_1 \neq l_2$). We first consider the case of $l_2 < l_1$. As shown in Fig. 8 the spontaneous emission spectrum changes dramatically in comparison with the symmetric-helicity case discussed above. As can be seen, a

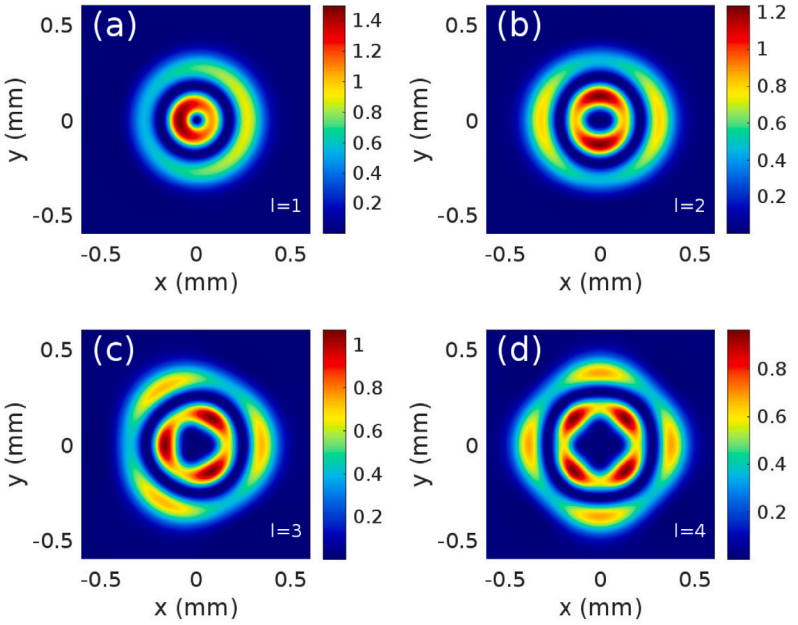

Fig. 5. Spatial modulation of the spontaneous emission $S(\delta_k)$ for initial condition $a_0(0) = 1/\sqrt{(2)}$, $a_1(0) = 1/\sqrt{(2)}$, $a_2(0) = 0$, $a_3(0) = 0$, for (a) $l = 1$, (b) $l = 2$, (c) $l = 3$, and (d) $l = 4$. Other parameters are $\delta_k = 0.04\Gamma$, $\Omega_p = 0.4\Gamma$, $\Omega_c = \Gamma$, $\Omega_m = 0.2\Gamma$; $\Delta_p = 2\Gamma$, $\Delta_c = 0$, and $\Delta_m = 0$.

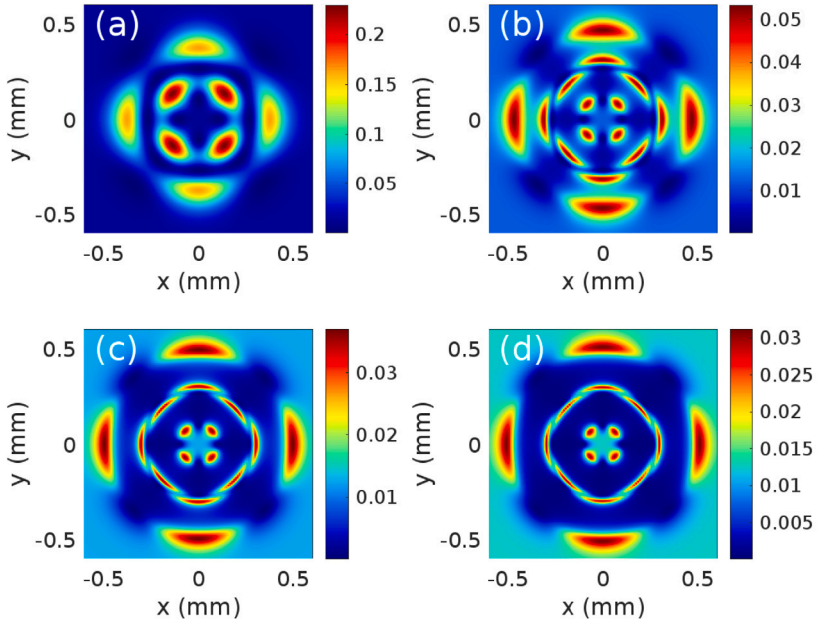

Fig. 6. Spatial modulation of the spontaneous emission $S(\delta_k)$ for initial condition $a_0(0) = 1/\sqrt{(2)}$, $a_1(0) = 1/\sqrt{(2)}$, $a_2(0) = 0$, $a_3(0) = 0$, $\delta_k = 0$, and l = 4 for different values of the detuning of the microwave field: (a) $\Delta_m = 0$, (b) $\Delta_m = 5\Gamma$, (c) $\Delta_m = 10\Gamma$, and (d) $\Delta_m = 15\Gamma$. Other parameters are $\Omega_p = 0.4\Gamma$, $\Omega_c = \Gamma$, $\Omega_m = 0.5\Gamma$, $\Delta_p = 2\Gamma$ and $\Delta_c = 0$.

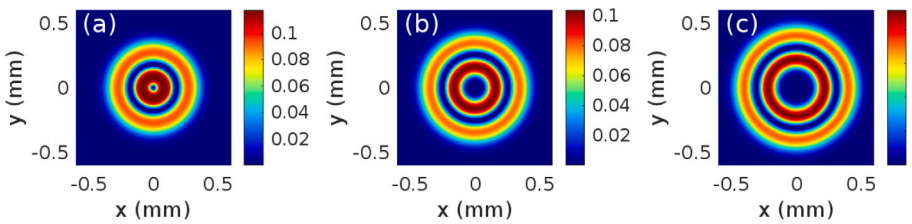

Fig. 7. Spatial modulation of the spontaneous emission $S(\delta_k)$ for initial condition $a_0(0) = 1/\sqrt{(2)}$, $a_1(0) = 1/\sqrt{(2)}$, $a_2(0) = 0$, $a_3(0) = 0$, $\delta_k = 0.3\Gamma$, wherein each control beams are implemented as vortex lights modulation with $l_1 = l_2$: (a) $l_1 = l_2 = 1$, (b) $l_1 = l_2 = 3$ and (c) $l_1 = l_2 = 5$. Other parameters are $\Omega_p = \Omega_c = \Gamma$, $\Omega_m = 0.5\Gamma$, $\Delta_p = 2\Gamma$ and $\Delta_p = \Delta_c = 0$.

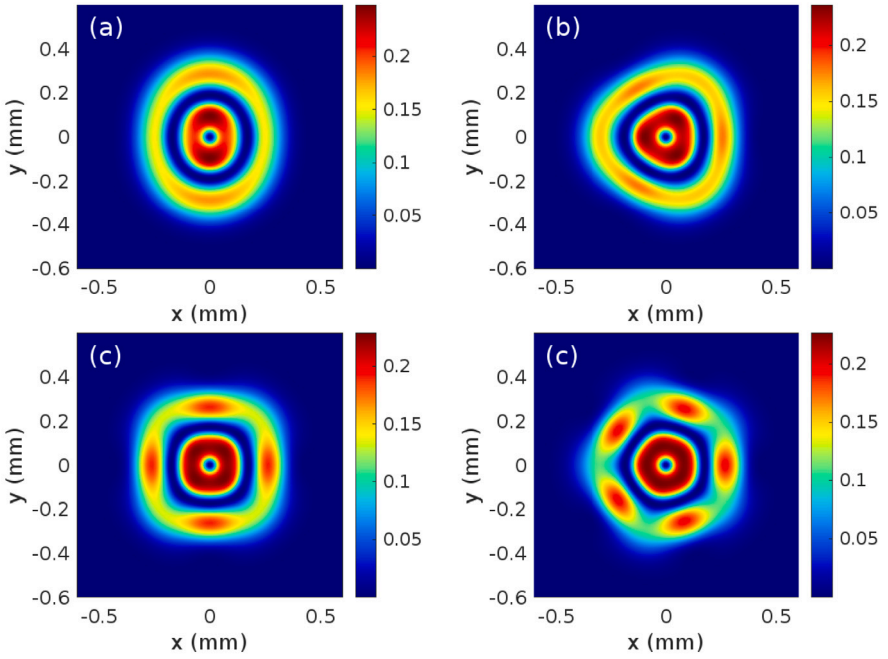

Fig. 8. Spatial modulation of the spontaneous emission $S(\delta_k)$ for initial condition $a_0(0) = 1/\sqrt{(2)}$, $a_1(0) = 1/\sqrt{(2)}$, $a_2(0) = 0$, $a_3(0) = 0$, $\delta_k = 0.3\Gamma$, wherein each control beams are implemented as vortex lights modulation with $l_2 < l_1$: (a) $l_1 = 3, l_2 = 1$, (b) $l_1 = 4, l_2 = 1$, (c) $l_1 = 5, l_2 = 1$ and (d) $l_1 = 6, l_2 = 1$. Other parameters are $\Omega_p = \Omega_c = \Gamma$, $\Omega_m = 0.5\Gamma$, $\Delta_p = 2\Gamma$ and $\Delta_m = \Delta_c = 0$.

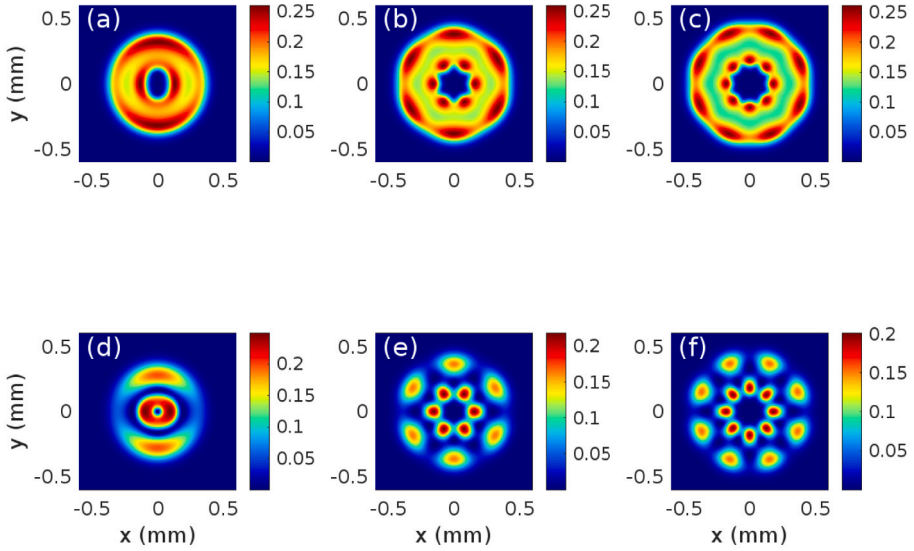

Fig. 9. Spatial spontaneous emission profile $S(\delta_k)$ for initial condition $a_0(0) = 1/\sqrt{(2)}$, $a_1(0) = 1/\sqrt{(2)}$, $a_2(0) = 0$, $a_3(0) = 0$, $\delta_k = 0.3\Gamma$, and wherein each control beams are implemented as vortex lights modulation: (a) $l_1 = 1, l_2 = -1$, (b) $l_1 = 3, l_2 = -3$, (c) $l_1 = 4, l_2 = -4$, (d) $l_1 = -1, l_2 = 1$, (e) $l_1 = -3, l_2 = 3$, and (f) $l_4 = -4, l_2 = 4$. Other parameters are $\Omega_p = \Omega_c = \Gamma$, $\Omega_m = 0.5\Gamma$, $\Delta_p = 2\Gamma$ and $\Delta_m = \Delta_c = 0$.

$|l_1 - l_2|$ fold rotational symmetry is found, showing $|l_1 - l_2|$ maxima as Eq. (15) predicts.

We now investigate the scenario in which the beams exhibit opposite vorticities, i.e., $l_1 = -l_2 = l$. It is worth noting that in this situation, the patterns of emission spectra depend on the sign of $l_1 - l_2 = 2l$, i.e., on the sign of l. For $l > 0$, the behavior can be explained from Eq. (15). In this case, this equation reduces to

$$S(\delta_k) = \frac{1}{2}\left|\frac{A^2|\Omega_p(l)|^2 + B^2|\Omega_c(-l)|^2 + 2AB|\Omega_p(l)||\Omega_c(-l)|\cos(2l\Phi)}{f(\delta_k)}\right|^2. \tag{16}$$

It can be seen from Eq. (16) that, although the interference term is independent of the sign of l, the intensity terms satisfy $A^2|\Omega_p(l)|^2 + B^2|\Omega_c(-l)|^2 \neq A^2|\Omega_p(-l)|^2 + B^2|\Omega_c(+l)|^2$, since $A \neq B$. In addition, the term $\cos(2l\Phi)$ introduces a $2l$-fold symmetry, resulting in a sinusoidal modulation of spontaneous emission patterns as shown in Figs. 9(a-f), but the width and the intensity differ when we change l by $-l$.

Finally, we analyze the effect of the microwave field for this case of two LG-mode control fields. Similarly to the case of one LG-mode control field, the spontaneous emission profile can be controlled by changing the Rabi frequency of the microwave field. Figs. 10(a)–(d) display the effect of increasing Ω_m for $l_1 = 3$ y $l_2 = -3$.

In absence of microwave field, ($\Omega_m = 0$), Fig. 10(a) displays a narrow double-ring structure while the overall intensity of the emitted light is very low. If the microwave field is set to a small value ($\Omega_m = 0.05\Gamma$), each ring breaks into $2l$ singularities, and the maximum intensity rises to five times higher values. A moderate increase of the Rabi frequency, $\Omega_m = 0.5\Gamma$, produces an enhancement of the

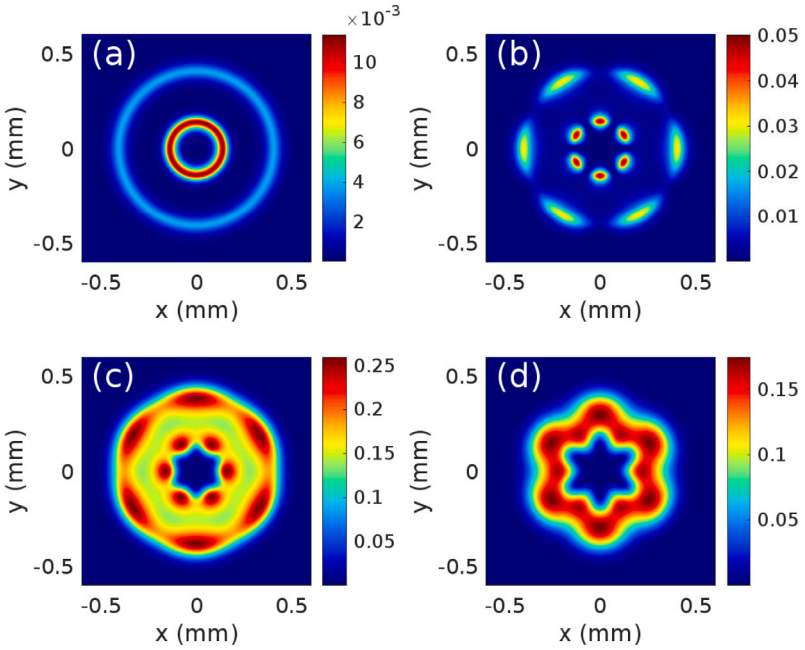

Fig. 10. Spatial modulation of the spontaneous emission $S(\delta_k)$ for initial condition $a_0(0) = 1/\sqrt{(2)}$, $a_1(0) = 1/\sqrt{(2)}$, $a_2(0) = 0$, $a_3(0) = 0$, for different values of the Rabi frequency of the microwave field in the case of two OAM field with $l_1 = -l_2 = 3$: (a) $\Omega_m = 0$, (b) $\Omega_m = 0.05\Gamma$, (c) $\Omega_m = 0.5\Gamma$, and (d) $\Omega_m = \Gamma$. Other parameters are $\Omega_p = \Omega_c = \Gamma$, $\Delta_p = 2\Gamma$, $\Delta_m = \Delta_c = 0$ and $\delta_k = 0.3\Gamma$.

spontaneous emission in the whole plane, but does not affect the overall pattern. Only the amplitude of the singularities is changed, as seen by comparing Figs. 10(b) and 10(c). However, a further increase of the Rabi frequency to $\Omega_m = \Gamma$ dramatically changes the spontaneous emission spatial distribution. A single ring star structure appears and a quenching of spontaneous emission takes place in the rest of the transverse plane.

The above obtained results point out that the proposed atomic scheme offers a wide range of tunability, i.e., one can manipulate the generated structured light fields by tuning the initial state of the atom, the topological charge of the control beams and the frequency and detuning of the auxiliary microwave field.

4. Summary

In summary, we have analyzed the generation of structured light via spontaneous emission in a five-level atomic system. Our approach shows that spatially dependent spontaneous emission spectra may be controlled by manipulating key parameters of the system: the strength of LG beams, the Rabi frequency and detuning of an external microwave field, and the initial state of the atoms. Moreover, we analyze the cases of one and two LG-mode beams interacting with the atom. It is found that due to these driving fields interference and their space-dependent intensity distribution, a variety of patterns in the spontaneous emission can arise, very different of original OAM driving fields. Specifically it is shown that structured spontaneous emission spectra may be generated through changing the values of the charge number l_j of the external incident fields. This enables quenching and enhancement of spontaneous emission in specific different azimuthal regions. The number of enhanced emission peaks in the emission patterns can also be controlled by changing the topological charge of the OAM beams.

Moreover, since no stringent conditions are required in our scheme to obtain vacuum induces coherences, the numerical results for atomic spontaneous emission may be observable in feasible experiments by using the ^87Rb atom in MOT, where the atomic temperature can be decreased to several tens of μK so that the Doppler broadening effect can be effectively eliminated. These investigations may find applications in the research related to structured light, for example, to store quantum information.

CRediT authorship contribution statement

M.A. Antón: Writing – review & editing, Writing – original draft, Visualization, Validation, Software, Methodology, Investigation, Formal analysis, Conceptualization. **E. Cabrera-Granado:** Writing – review & editing, Validation, Software, Investigation.

Declaration of competing interest

The authors declare that they have no known competing financial interests or personal relationships that could have appeared to influence the work reported in this paper.

Acknowledgment

The authors acknowledge funding from Proyectos de Generación de Conocimiento 2022 call of the Ministerio de Ciencia e Innovación, project reference PID2022-136260NB-I00

Appendix. Calculation of the dressed states of the atomic system

Some of results obtained numerically in the preceding section can be interpreted in the atom-field dressed representation. It is well known that the positions, widths and heights of resonance fluorescence peaks can be understood through energies, electronic dipole moments and steady-state populations of the dressed states.

The dressed states produced by the driving control field Ω_c and the microwave field Ω_m, which couple the transitions $|1\rangle$, $|2\rangle$, and $|3\rangle$,

are obtained by finding the eigenvectors of the coherent part of the interaction Hamiltonian, Eq. (2), i.e., we must solve

$$H_c|\psi_i\rangle = \lambda_i|\psi_i\rangle\,, \tag{17}$$

where H_c is given by the coherent part of the Hamiltonian

$$\begin{aligned} H_c &= \hbar\left[\Delta_p\sigma_{33} + (\Delta_p-\Delta_c)\sigma_{22} + (\Delta_p-\Delta_c-\Delta_m)\sigma_{11} + (\Delta_p-\delta_k)\sigma_{ee}\right] \\ &\quad + \hbar\left(\Omega_c\sigma_{32} + \Omega_m\sigma_{21} + H.c.\right)\,, \end{aligned} \tag{18}$$

The eigenvalues λ_i satisfy the equation

$$\begin{aligned} &\left(\Delta_p-\Delta_c-\Delta_m-\lambda\right)\left(\Delta_p-\lambda\right)\left(\Delta_p-\Delta_c-\lambda_i\right) - |\Omega_c|^2\left(\Delta_p-\delta_k-\lambda_i\right) \\ &- |\Omega_m|^2(\Delta_p-\lambda_i) = 0 \end{aligned} \tag{19}$$

In order to obtain the dressed states under arbitrary parametric conditions, we have to resort to numerical methods due to the complexity of the Eq. (19). However, under special circumstances we can look for the analytical solutions. The simplest situation is $\Delta_p = \delta_k = 0$. In this case, Eq. (19) reads

$$\lambda_b = 0 \quad ; \quad \lambda_\pm = \frac{\Delta_m \pm \sqrt{\Delta_m^2 + 4(\Omega_c^2+\Omega_m^2)}}{2}\,. \tag{20}$$

The corresponding eigenstates are given by

$$|\psi_i\rangle = C_{i1}|1\rangle + C_{i2}|2\rangle + C_{i3}|3\rangle \ (i=+,b,-)\,. \tag{21}$$

where the coefficients C_{ij} $(j=1,2,3)$ are

$$\begin{aligned} C_{i1} &= \frac{\Omega_m^*}{\sqrt{|\Omega_m|^2+|\Omega_c|^2+\lambda_i^2}}\,, \\ C_{i2} &= \frac{\lambda_i}{\sqrt{|\Omega_m|^2+|\Omega_c|^2+\lambda_i^2}}\,, \\ C_{i3} &= \frac{\Omega_c}{\sqrt{|\Omega_m|^2+|\Omega_c|^2+\lambda_i^2}}\,, \end{aligned} \tag{22}$$

It can clearly be seen that the dressed states form a ladder of triplets as shown in Fig. 1(b) with probability amplitudes depending on the Rabi frequencies of the control field Ω_c and the microwave field Ω_m. In addition, a lengthy but straightforward calculation allows us to express the equation of temporal evolution of the amplitudes appearing in Eqs. (5) in the dressed state representation as

$$\begin{aligned} \frac{\partial a_0(t)}{\partial t} &= -i\Omega_{p+}a_+(t) - i\Omega_{pb}a_b(t) - i\Omega_{p-}a_-(t), \\ \frac{\partial a_+(t)}{\partial t} &= -\left[\Gamma_+/2 + i(\Delta_p+\lambda_+)\right]a_+(t) - i\Omega_{p+}^*a_0(t) - \frac{\sqrt{\Gamma_+\Gamma_-}}{2}a_-(t) - \frac{\sqrt{\Gamma_+\Gamma_b}}{2}a_b(t), \\ \frac{\partial a_b(t)}{\partial t} &= -\left[\Gamma_b/2 + i\Delta_p\right]a_b(t) - i\Omega_{pb}^*a_0(t) - \frac{\sqrt{\Gamma_b\Gamma_+}}{2}a_+(t) - \frac{\sqrt{\Gamma_b\Gamma_-}}{2}a_-(t)\,, \\ \frac{\partial a_-(t)}{\partial t} &= -\left[\Gamma_-/2 + i(\Delta_p+\lambda_-)\right]a_-(t) - i\Omega_{p-}^*a_0(t) - \frac{\sqrt{\Gamma_-\Gamma_+}}{2}a_+(t) - \frac{\sqrt{\Gamma_-\Gamma_b}}{2}a_b(t)\,, \\ \frac{\partial a_k(t)}{\partial t} &= -i\left(\Delta_p-\delta_k\right)a_k(t) - ig_{k+}^*a_+(t) - ig_{kb}^*a_b(t) - ig_{k-}^*a_-(t)\,, \end{aligned} \tag{23}$$

where the effective Rabi frequency are $\Omega_{p+} = \Omega_p\Omega_c/\sqrt{|\Omega_m|^2+|\Omega_c|^2+\lambda_+^2}$, $\Omega_{pb} = \Omega_p\Omega_m/\sqrt{|\Omega_m|^2+|\Omega_c|^2}$ and $\Omega_{p-} = \Omega_p\Omega_c/\sqrt{|\Omega_m|^2+|\Omega_c|^2+\lambda_-^2}$. On the other hand the decay rates from the dressed atomic levels to the metastable level are given by

$$\begin{aligned} \Gamma_+ &= \frac{|\Omega_c|^2\Gamma}{|\Omega_m|^2+|\Omega_c|^2+\lambda_+^2}\,, \\ \Gamma_b &= \frac{|\Omega_m|^2\Gamma}{|\Omega_m|^2+|\Omega_c|^2}\,, \\ \Gamma_- &= \frac{|\Omega_c|^2\Gamma}{|\Omega_m|^2+|\Omega_c|^2+\lambda_-^2}. \end{aligned} \tag{24}$$

An inspection of Eqs. (23) and (24) shows that: (1) the current atomic system is equivalent to a five-level atomic system with vacuum induced coherence since the terms depending on $\sqrt{\Gamma_+\Gamma_b}$, $\sqrt{\Gamma_-\Gamma_b}$ and $\sqrt{\Gamma_+\Gamma_-}$, etc, in Eqs(23) clearly show that spontaneous emission from the dressed excited levels can interfere, and (2) these terms can be modulated by the Rabi frequency of the control and microwave fields, as can be seen from Eqs. (24). Thus, the current system is equivalent to a system with vacuum induced coherence as investigated in Ref. [55], but the three close-lying levels are dressed states instead of real states. This is a good property of the proposed atomic system since it mimics a system with VIC without the need for specific and difficult conditions to be fulfilled in real systems.

Data availability

Data will be made available on request.

References

[1] Y. Arita, E.W. M. Chen and, K. Dholakia, Dynamics of a levitated microparticle in vacuum trapped by a perfect vortex beam: Three- dimensional motion around a complex optical potential, J. Opt. Soc. Am. B 34 (2017) C14, http://dx.doi.org/10.1364/josab.34.000c14.

[2] Y. Liang, M. Lei, S. Yan, M. Li, Y. Caiand, Z. Wang, Rotating of low-refractive index microparticles with a quasi-perfect optical vortex, Appl. Opt. 57 (2018) 79, http://dx.doi.org/10.1364/AO.57.000079.

[3] H. Yan, E. Zhang, B. Zhaoand, K. Duan, Free-space propagation of guided optical vortices excited in an annular core fiber, Opt. Express 20 (2012) 17904, http://dx.doi.org/10.1364/OE.20.017904.

[4] J. Leach, J. Romero, A. Yao, S. Franke-Arnold, Quantum correlations in optical angle-orbital angular momentum variables, Science (2010) 329, http://dx.doi.org/10.1126/science.1190523.

[5] R. Fickler, R. Lapkiewicz, W. Plick, M. Krenn, C. Schaeff, et al., Quantum entanglement of high angular momenta, Science 338 (2012) 640, http://dx.doi.org/10.1126/science.1227193.

[6] A. Nicolas, L. Veissier, L. Giner, E. Giacobino, J. Laurat, Quantum memory for orbital angular momentum photonic qubits, Nat. Photon 8 (2014) 234, http://dx.doi.org/10.1038/nphoton.2013.355.

[7] L. Allen, M. Beijersbergen, R. Spreeuw, J.P. Woerdman, Orbital angular momentum of light and the transformation of laguerre-Gaussian laser modes, Phys. Rev. A 45 (1992) 8185, http://dx.doi.org/10.1103/PhysRevA.45.8185.

[8] M. Padgett, J. Courtial, L. Allen, Light's orbital angular momentum, Phys. Today 57 (2004) 35, http://dx.doi.org/10.1063/1.1768672.

[9] L. Deng, M.G. Payne, W.R. Garrett, Effects of multi-photon interferences from internally generated fields in strongly resonant systems, Phys. Rep. 429 (2006) 123, http://dx.doi.org/10.1364/OE.447397.

[10] Harris, Nonlinear optical processes using electromagnetically induced transparency, Phys. Rev. Lett. 64 (1990) 1107, http://dx.doi.org/10.1103/PhysRevLett.64.1107.

[11] Fleischhauer, et al., Resonantly enhanced refractive index without absorption via atomic coherence, Phys. Rev. A 46 (1992) 1468, http://dx.doi.org/10.1103/PhysRevA.46.1468.

[12] Fleischhauer, et al., Electromagnetically induced transparency: optics in coherent media, Rev. Modern Phys. 77 (2005) 633, http://dx.doi.org/10.1103/RevModPhys.77.633.

[13] M.O. Scully, et al., Lasers without inversion, Phys. Rev. Lett. 263 (1994) 337, http://dx.doi.org/10.1126/science.263.5145.337.

[14] J. Ruseckas, A. Mekys, G. Juzeliunas, Slow polaritons with orbital angular momentum in atomic gases, Phys. Rev. A 83 (2011) 023812, http://dx.doi.org/10.1103/PhysRevA.83.023812.

[15] J. Ruseckas, V. Kudriasov, I.A. Yu, G. Juzeliunas, Transfer of orbital angular momentum of light using two-component slow light, Phys. Rev. A 87 (2013) 053840, http://dx.doi.org/10.1103/PhysRevA.87.053840.

[16] H. Hamedi, A. Khaledi-Nasab, A. Raheli, Kerr nonlinearity and EIT in a double lambda type atomic system, Opt. Spectrosc. 115 (2013) 544, URL https://doi.org/10.1134/S0030400X13100056.

[17] H.R. Hamedi, J. Ruseckas, E. Paspalakis, G. Juzeliunas, Transfer of optical vortices in coherently prepared media, Phys. Rev. A 99 (2019) 033812, URL https://doi.org/10.1103/PhysRevA.99.033812.

[18] C. Yu, Z. Wang, Engineering helical phase via four-wave mixing in the ultraslow propagation regime, Phys. Rev. A 103 (2021) 013518, URL https://doi.org/10.1103/PhysRevA.103.013518.

[19] Y. Hong, Z. Wang, D. Ding, B. Yu, Ultraslow vortex four-wave mixing via multiphoton quantum interference, Opt. Express 27 (2019) 29863, URL https://doi.org/10.1364/OE.27.029863.

[20] Y. Zhang, Z. Wang, J. Qiu, Y. Hong, B. Yu, Spatially dependent four-wave mixing in semiconductor quantum wells, Appl. Phys. Lett. 115 (2019) 171905, URL https://doi.org/10.1063/1.5121275.

[21] D. Moretti, D. Felinto, J.W.R. Tabosa, Collapses and revivals of stored orbital angular momentum of light in a cold-atom ensemble, Phys. Rev. A 79 (2009) 023825, URL https://doi.org/10.1103/PhysRevA.79.023825.
[22] J. Qiu, Z. Wang, D. Ding, W. Li, B. Yu, Highly efficient vortex four-wave mixing in asymmetric semiconductor quantum wells, Opt. Express 28 (2020) 2975, URL http://doi.og/10.1364/OE.379245.
[23] J.R. H. R. Hamedi, G. Juzeliunas, Exchange of optical vortices using an electromagnetically-induced-transparency–based four-wave-mixing setup, Phys. Rev. A 98 (2018) 013840, URL https://doi.org/10.1103/PhysRevA.98.013840.
[24] S. Hawkins, E. Gansen, M. Stevens, A. Smirl, I. Rumyantsev, R. Takayama, N. Kwong, R. Binder, D. Steel, Differential measurements of Raman coherence and two-exciton correlations in quantum wells, Phys. Rev. B 68 (2003) 035313, URL https://doi.org/10.1103/PhysRevB.68.035313.
[25] A. Imamoglu, Electromagnetically induced transparency with two dimensional electron spins, Opt. Commun. 179 (2000) 035313, URL https://doi.org/10.1016/S0030-4018(99)00667-7.
[26] M. Phillips, H. Wang, I. Rumyantsev, N. Kwong, R. Takayama, R. Binder, Electromagnetically induced transparency in semiconductors via biexciton coherence, Phys. Rev. Lett. 91 (2003) 183602, URL https://doi.org/10.1103/PhysRevLett.91.183602.
[27] Z. Wang, Y. Zhang, E. Paspalakis, B. Yu, Efficient spatiotemporal-vortex four-wave mixing in a semiconductor nanostructure, Phys. Rev. A 102 (2020) 063509, URL, https://doi.org/10.1103/PhysRevA.102.063509.
[28] J. Qiu, Z. Wang, D. Ding, W. Li, B. Yu, Highly efficient vortex four-wave mixing in asymmetric semiconductor quantum wells, Opt. Express 28 (2020) 2975, [URL, https://doi.org/10.1364/OE.379245.
[29] Rahmatullah, M. Abbas, Ziauddin, S. Qamar, Spatially structured transparency and transfer of optical vortices via four-wave mixing in a quantum-dot nanostructure, Phys. Rev. A 101 (2020) 023821, URL https://doi.org/10.1103/PhysRevA.101.023821.
[30] H. Hamedi, J. Ruseckas, G. Juzeliunas, Phys. Rev. A 98 (2018) 013840, http://dx.doi.org/10.1103/PhysRevA.98.013840, URL link.
[31] H. Hamedi, J. Ruseckas, E. Paspalakis, G. Juzeliunas, Off-axis optical vortices using double-Raman singlet and doublet light-matter schemes, Phys. Rev. A 101 (2020) 063828, URL https://doi.org/10.1103/PhysRevA.101.063828.
[32] H. Hamedi, G. Zlabys, V. Ahufinger, T. Halfmann, J. Ruseckas, G. Juzeliunas, Spatially strongly confined atomic excitation via a two dimensional stimulated Raman adiabatic passage, Opt. Express 30 (2022) 13915, URL https://doi.org/10.1364/OE.447397.
[33] Y. Chao, Z. Wang, Engineering helical phase via four-wave mixing in the ultraslow propagation regime, Phys. Rev. A 103 (2021) 013518, URL https://doi.org/10.1103/PhysRevA.103.013518.
[34] L. Ding, F. Wang, F. Hu, Raman-induced transfer of optical vortices, Laser Phys. Lett. 19 (2022) 035208, URL https://doi.org/10.1088/1612-202X/ac5047.
[35] M. Mahdavi, Z. Sabegh, H. Hamedi, M. Mahmoudi, Orbital angular momentum transfer in molecular magnets, Phys. Rev. B 104 (2021) 094432, URL https://doi.org/10.1103/PhysRevB.104.094432.
[36] J.L. C. Ding and, X. Dai, R. Jin, X. Hao, Azimuthal and radial modulation of double-four-wave mixing in a coherently driven graphene ensemble, Opt. Express 29 (2021) 36840, URL https://doi.org/10.1364/OE.440690.
[37] S.Y. Zhu, M.O. Scully, Spectral line elimination and spontaneous emission cancellation via quantum interference, Phys. Rev. Lett. 76 (1996) 388, URL https://doi.org/10.1103/PhysRevLett.76.388.
[38] Z. Ficek, S. Swain, Quantum interference in optical fields and atomic radiation, J. Modern Opt. 49 (2002) 3, URL https://doi.org/10.1080/09500340110065781.
[39] L.M. Narducci, M.O. Scully, G.L. Oppo, P. Ru, J.R. Tredicce, Spontaneous emission and absorption properties of a driven three-level system, Phys. Rev. A 42 (1990) 1630, URL https://doi.org/10.1103/PhysRevA.42.1630.
[40] K.T. Kapale, M.O. Scully, S. Zhu, M.S. Zubairy, Quenching of spontaneous emission through interference of incoherent pump processes, Phys. Rev. A 67 (2003) 023804, URL https://doi.org/10.1103/PhysRevA.67.023804.
[41] M.A. Antón, O.G. Calderón, F. Carreño, Spontaneously generated coherence effects in a laser-driven four-level atomic system, Phys. Rev. A 72 (2005) 023809, URL https://doi.org/10.1103/PhysRevA.72.023809.
[42] E. Paspalakis, P.L. Knight, Phase control of spontaneous emission, Phys. Rev. Lett. 47 (2000) 1025, URL https://doi.org/10.1103/PhysRevLett.81.293.
[43] L.F. Li, Z. Shi-Yao, Resonance fluorescence quenching and spectral line narrowing via quantum interference in a four-level atom driven by two coherent fields, Phys. Rev. A 59 (1999) 2330, URL https://doi.org/10.1103/PhysRevA.59.2330.
[44] D. Bullock, J. Evers, C.H. Keitel, Modifying spontaneous emission via interferences from incoherent pump fields, Phys. Lett. A 307 (2003) 8, URL https://doi.org/10.1016/S0375-9601(02)01667-5.
[45] G.S. Agarwal, P.K. Pathak, Dc-field-induced enhancement spontaneous emission in a cavity, Phys. Rev. A 70 (2004) 025802, 10.1103/physreva.70.025802.
[46] S. John, T. Quang, Collective switching and inversion without fluctuation of two-level atoms in confined photonic systems, Phys. Rev. Lett. 78 (1997) 1888, URL https://doi.org/10.1103/PhysRevLett.78.1888.
[47] S. Evangelou, V. Yannopapas, E. Paspalakis, Modifying free-space spontaneous emission near a plasmonic nanostructure, Phys. Rev. A 83 (2011) 023819, URL https://doi.org/10.1103/PhysRevA.83.023819.
[48] M. Abbas, U.S. Rahmatullah, Y.-C. Zhang, P. Zhang, Spontaneously generated structured light in a coherently driven five-level M-type atomic system, Phys. Rev. A 109 (2024) 023716, http://dx.doi.org/10.1103/PhysRevA.109.023716.
[49] S.H. Asadpour, M. Abbas, H.R. Hamedi, J. Ruseckas, E. Paspalakis, R. Asgari, Spatiospectral control of spontaneous emission, Phys. Rev. A. 110 (2024) 033706, http://dx.doi.org/10.1103/PhysRevA.110.033706.
[50] L. Jia-Hua, L.J. Bing, C. Ai-Xi, Q. Chun-Chao, Spontaneous emission spectra and simulating multiple spontaneous generation coherence in a five-level atomic medium, Phys. Rev. A 74 (2006) 033816, http://dx.doi.org/10.1103/PhysRevA.74.033816.
[51] M. Abbas, S.H. Asadpour, Rahmatullah, F. Wang, H.R. Hamedi, P. Zhang, Azimuthally dependent spontaneous emission from a coherently microwave-field driven four-level atom-light coupling scheme, Chaos Solitons Fractals (ISSN: 0960-0779) 189 (2024) 115672, http://dx.doi.org/10.1016/j.chaos.2024.115672, URL https://www.sciencedirect.com/science/article/pii/S0960077924012244.
[52] Z. Wang, K. Marzlin, B. Sanders, Large cross-phase modulation between slow copropagating weak pulses in 87Rb, Phys. Rev. Lett. 97 (2006) 063901, http://dx.doi.org/10.1103/PhysRevLett.97.063901.
[53] S.M. Barnet, P.M. Radmore, Methods in theoretical Quantum Optics, Cambridge University Press, Oxford, 2000.
[54] D. Steck, 87Rb D Line Dat, URL http://steck.us/alkalidata.
[55] A. Fountoulakis, A.F. Terzis, E. Paspalakis, Coherent phenomena due to double-dark states in a system with decay interference, Phys. Rev. A 73 (2006) 033811, http://dx.doi.org/10.1103/PhysRevA.73.033811.